Saturation limits for the PACS Photometer

M. Sauvage, N. Billot, K. Okumura

Document Change Record			
Version	Date	Author	Change description
0.1	June 5, 2008	MS	Creation of the document.
0.2	July 4, 2008	MS, KO, NB	Major restructuring (now CL section is first), and making a more extensive use of ILT data.
1.0	July 22, 2008	MS	Incorporated comments from first broad circulation. Took into account uncertainties in ADC saturation which led to an increase of the saturation limit in ADC regime. Added appendix A (single setting on the blue photometer), and B (saturation on the most forgiving blue areas).

Reference documents			
Ref.	ID	Version	Title
RD1	SAp-PACS-MS-0616-06	Draft 9	PACS FM Photometer Focal Plane Unit Users Manual
RD2	PICC-ME-TR-006	0.1	PACS test analysis report FM-ILT
RD3	SAp-PACS-MS-0305-04	2.0	Backgrounds, noises and sensitivities
RD4	SAp-PACS-NB-0671-07	n.a.	Nicolas Billot's PhD thesis

Abstract

This note is devoted to the computation of the saturation limits for each band of the PACS photometer and for each setting of the user-selectable gain. Because the actual background is unknown, we also compute these limits for plausible values of the telescope flux. We show that saturation is a far more complex issue than what most people (including the present authors) envision, and that it takes on many new faces in the context of a bolometer instrument such as PACS. For those only interested in the results, we show that for a reasonable value of the background, i.e. 2.0 pW/pix, the point source saturation limits stand at 290, 680, 1280 Jy for respectively the blue, green, and red bands at high gain, and at 445, 1040, and 1860 Jy for the blue, green and red bands at low gain (many more numbers are given in Table 13, but no strong variation with background level are observed. The numbers quoted here assume an independent detector setup for the blue and green filters, see Appendix A for a discussion of this aspect). If you have trouble figuring out why these numbers are what they are, read on (although we do not guarantee that things will be clearer in the end). Note that we only consider here saturation introduced by the analog-to-digital converter and the readout circuit. There is a third way to saturate a bolometer: expose it to so much flux that its response goes down to zero. It turns out that in all realistic situations, this regime will not be reached.

Contents

1 Purpose and some definitions

The question of which flux level leads to photometer saturation, with its associated misconceptions, has now come up sufficiently often that writing a (not so) short note about it is probably a good idea.

First what do we mean by saturation (and bolometer experts may indeed be puzzled)? A bolometer cannot saturate in the same way a photoconductor or a CCD does. As the flux of the sources we observe increases, the response of a bolometer decreases, up to a point where the flux is driving it so hot that the signal does not change anymore. This "saturation" of the responsivity is not what we are computing here. It has been measured during FM-ILT and we will use it instead. We concentrate here on saturation limits introduced by the instrument's electronics: the PACS bolometer are read by a system that, among other things carries the signal from the bolometer to the observer and converts the analog signal into a digitized information. These two steps can lead to effective "saturation", i.e. a loss of the system's capacity to respond to flux variations above a certain threshold.

First when the incoming flux is such that the voltage at the thermally variable resistor, i.e. the bolometer voltage, drops below $\approx$250 mV[1], the readout circuit becomes unable to carry it. This is called the readout circuit saturation, or the CL saturation to use RD1 notations. Second, the dynamical range available to digitize the signal is actually limited by the 16-bit AD converter of the warm electronics, and thus this defines a range of analog signals that can be transmitted, this is the ADC saturation. Determining the saturation limits amounts to figuring out which of these two effects happens first and for which source flux. Things are made a bit more complex by the fact that most of the signal is due to the telescope background, and that the bolometer matrices are very inhomogenous, i.e. a large fraction of the available dynamical range is used by the background and not by the source (see Figure 1). Note that we avoid reaching the 250 mV limit on the background itself by using an "educated" choice of the bolometer polarizing bias.

Finally, one should remember that bolometers are non-linear detectors, and that has to be taken into account to derive saturation limits expressed in power units (pW/pixels, Jy) rather than in signal units (V). This is where the "saturation" of the response can come into play.

In this document we shall first compute the voltage range that is available for the source signal in the different configurations of the photometer, first in the case of the CL saturation, and then in the case of the ADC saturation. The actual saturation limit corresponds, for each configuration, to the smallest value of the ADC and CL ranges. We have to proceed for the two effects independently as making a single formulation would render this note too complex to follow. While doing so, we will assume that the detectors can be tuned independently for blue and green observations (this will become clear later on). This is not the current baseline for the photometer operation and we will study the impact of a single tuning for blue and green observations at the end of this note. When the final voltage range available for sources is computed, we will turn it into a flux limit expressed in more conventional astronomical units than Volts or Watts per pixel.

2 The CL saturation

This is a complex computation because the readout circuit is a complex beast. The CL saturation comes from the fact that only those bolometer signals that are within a certain absolute range can be transmitted by the readout circuit. This has been brillantly shown in RD4 where we see (p. 102) the electronics gain catastrophically dropping for voltages higher than $\sim$650 mV or lower than $\sim$250 mV

[1] The system is such that a flux increase corresponds to a bolometer voltage decrease. Note that there is also an upper limit to the voltage than can go through the readout circuit, see Section 2.

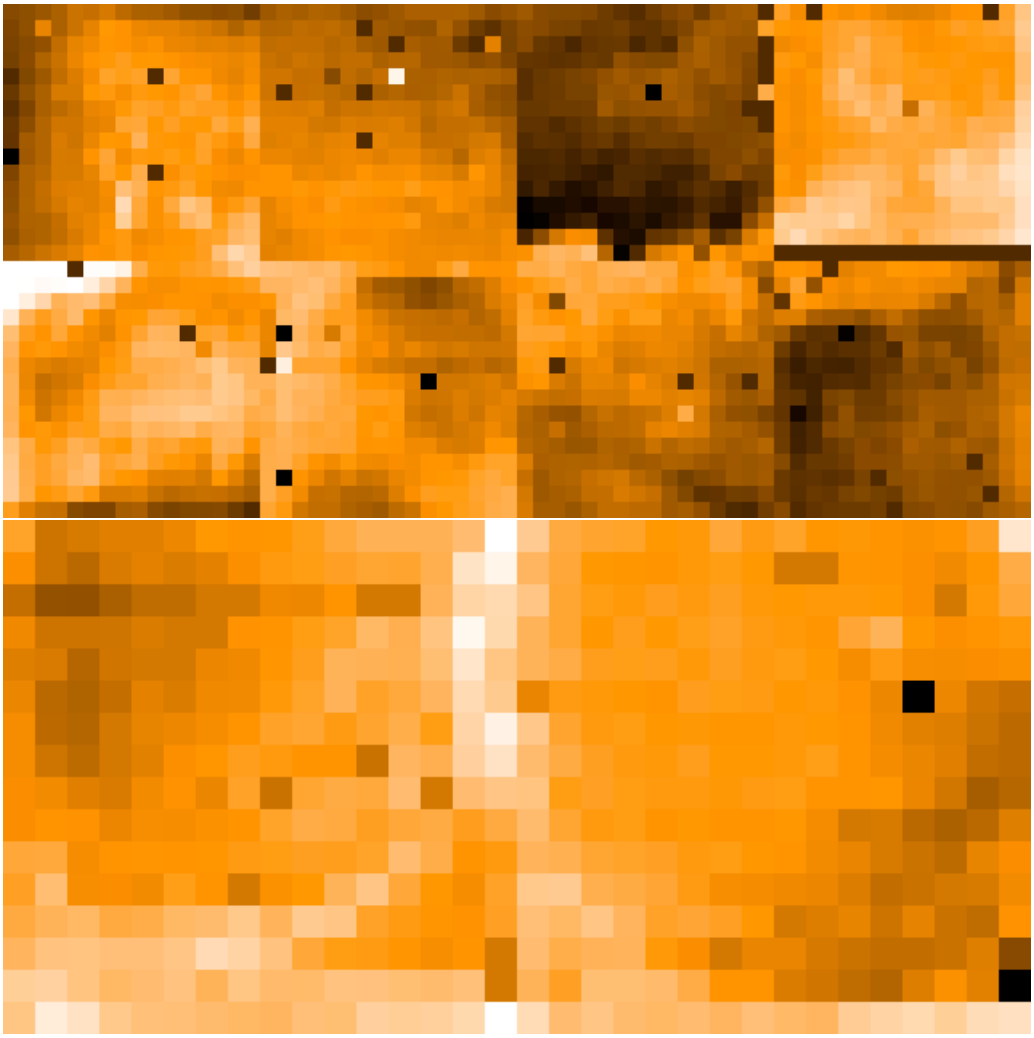

Figure 1: The aspect of the blue focal plane (top) and red focal plane (bottom) when illuminated by a flat source. What is shown here is the value of the signal in the telemetry. This image is obtained with an optimal setup for each group with respect to its own dispersion and the requirement to allow the largest possible range for source signals. Areas that appear dark under this optimal setting are those where the brightest sources could be allowed. Areas that appear light, or even white, are close to saturation already.

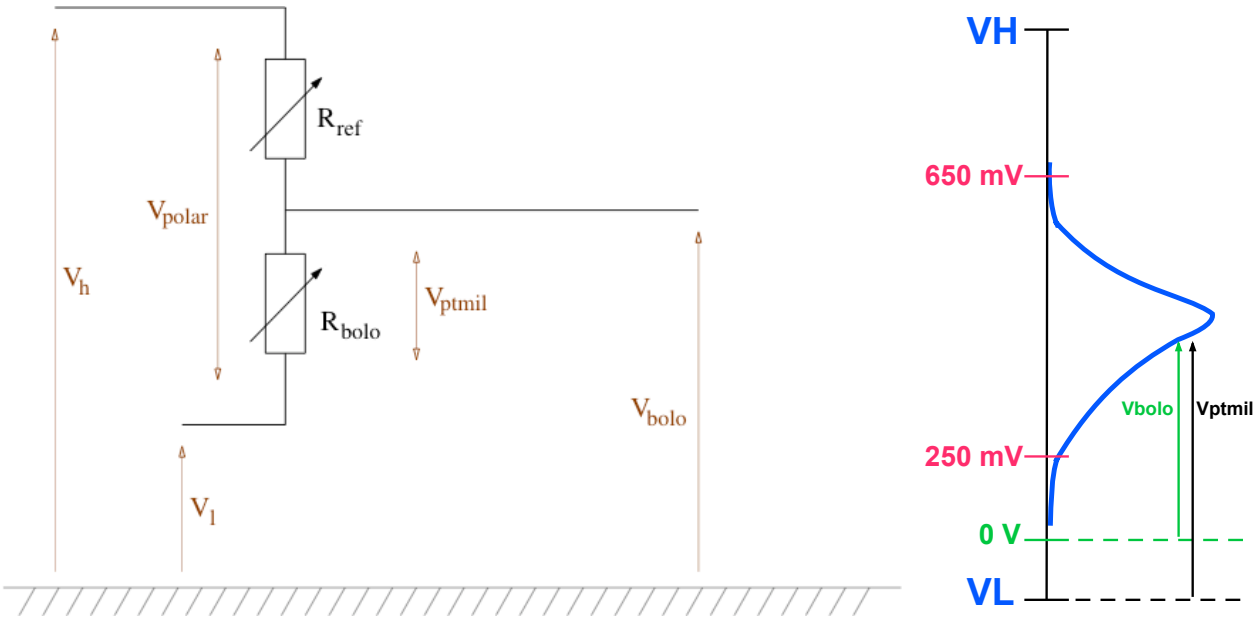

Figure 2: *Left:* A sketch (from RD4) of the bolometer circuit defining the polarization biases and signals. As you know, both resistors are identical but the reference resistor is thermalized. The values of V_H and V_L are controled individually, but V_L can never be positive. The signal that we measure is V_{bolo}, it is that signal that has to fit into the [250, 650] mV range to be carried through the readout circuit. As is evident from the figure, the value V_{bolo} is influenced by V_L: as V_L is negative by contruction, it is smaller than V_{ptmil}, the voltage at the middle point of the bolometer bridge. *Right:* a sketch of how the signal is distributed. By constrution of the system, the signal at the middle point of the bolometer bridge is comprised between V_H and V_L. Changing the values of theses biases streches or compresses this distribution (when each bias is modified individually) or globally moves this distribution (when both are modified while keeping their difference constant). However the parts of the distribution that fall below 250 mV or above 650 mV will be lost in the readout process. As V_L cannot be positive, and we want to preserve as much of the full signal distribution, cases will occur when the actual signal cannot be brought above 250 mV, i.e. we saturate in the CL.

(this latter limit corresponding to the high flux limit). These are hard limits, and the range they define cannot be modified by means of some bias changes. Since we intend to compute numerical values for the flux limits, we need to arbitrarily define what we consider as the acceptable range for the CL. Looking at RD4 we see that the CL gain variations are minimal (i.e. the gain varies from 0.95 to 0.97) over the range [250, 650] mV, and this is now the range where we want to place all the photometer signals.

The reason it is complex to translate these limits into a source flux is that we now have to actually compute the exact signal voltage corresponding to the background and source, i.e. we have to take into account detector physics. To clarify how we are going to do this let's go back to the basics, following the luminous path of RD4.

2.1 The bolometers

Figure 2 (left panel) shows a sketch of the bolometer bridge (taken from N. Billot's PhD thesis, RD4), where the different biases and voltages can be identified. Biasing the detector means setting V_H and

V_L to predefined values (with V_L being negative by construction of the electronics, this has been relaxed for the next generation of instruments using these detectors). Exposing the bolometer resistor to light changes its value and the voltage at the middle point of the bolometer bridge can be expressed as:

$$V_{ptmil} = \frac{R_{bolo}}{R_{bolo} + R_{ref}} \times (V_H - V_L). \quad (1)$$

This resistor ratio is called the RR ratio in inner bolometer circles and its behavior, or equivalently as we will use here that of V_{ptmil}, as a function of the polarization bias $(V_H - V_L)$ and of the incoming flux (P_{bkg}) has been the subject of extensive measurements during FM-ILT. The resulting curves can be found in RD4 (specifically p.106) or RD2. These curves, i.e. $V_{ptmil}(P_{bkg}, V_{polar})$ where P_{bkg} is the background power per pixel, and $V_{polar} = (V_H - V_L)$, can be fitted to provide us with a statistical description of the V_{ptmil} distribution, $\langle V^{blue}_{ptmil}(P_{bkg})\rangle$, $\sigma_{V^{blue}_{ptmil}}(P_{bkg})$, $\langle V^{red}_{ptmil}(P_{bkg})\rangle$, $\sigma_{V^{red}_{ptmil}}(P_{bkg})$, i.e. the mean and standard deviation value for the V_{ptmil} curve as a function of background only, as $(V_H - V_L)$ is fixed (this is the optimal polarization) per photometer side, that we can then use to derive the CL saturation limit. This approach however assumes that the distribution of middle point values on a group (because we can only tune polarizations on a group basis) can satisfactorily be described by a gaussian. This is unfortunately not the case, the extreme example being group 4, where the two matrices are so distinct that the distribution of V_{ptmil} observed for a flat illumination is double-peaked. Therefore we rather use the FM-ILT measurements to measure $\Delta V_{ptmil}(P_{bkg})$ and $V^{Max}_{ptmil}(P_{bkg})$, respectively the total extent and the maximum value of the V_{ptmil} distribution as a function of the background level. For the purpose of computing a saturation limit, we only have to measure these for the most dispersed group per band. This is group 1 on the blue side and group 6 on the red side. The actual distribution of the middle point values as a function of background for these two groups is shown on Figure 3 while Table 1 lists the measured $\Delta V_{ptmil}(P_{bkg})$ and $V^{Max}_{ptmil}(P_{bkg})$.

Table 1: Total dispersion of the middle point values observed on group 1 (blue) and group 6 (red), the most dispersed groups, as a function of background illumination, accompanied by the maximum observed middle point value on these groups. This shows that as the flux increases, the distribution of middle point values spreads out, while the whole distribution shifts downward.

Background level (pW/pix)	Group 1 (Blue)		Group 6 (Red)	
	$\Delta V_{ptmil}(P_{bkg})$ (V)	$V^{Max}_{ptmil}(P_{bkg})$ (V)	$\Delta V_{ptmil}(P_{bkg})$ (V)	$V^{Max}_{ptmil}(P_{bkg})$ (V)
1.0	0.277	0.985	0.133	0.900
2.0	0.293	0.962	0.159	0.873
3.0	0.310	0.946	0.179	0.849
4.0	0.306	0.914	0.195	0.827
5.0	0.323	0.904	0.208	0.805
6.0	0.321	0.877	0.218	0.785
7.0	0.319	0.851	0.226	0.766

2.2 Expressing the saturation condition

The signal will "saturate" the CL either if it falls below 250 mV or if it rises above 650 mV. How can we turn that sentence into an equation? This is now relatively straightforward, we simply want to

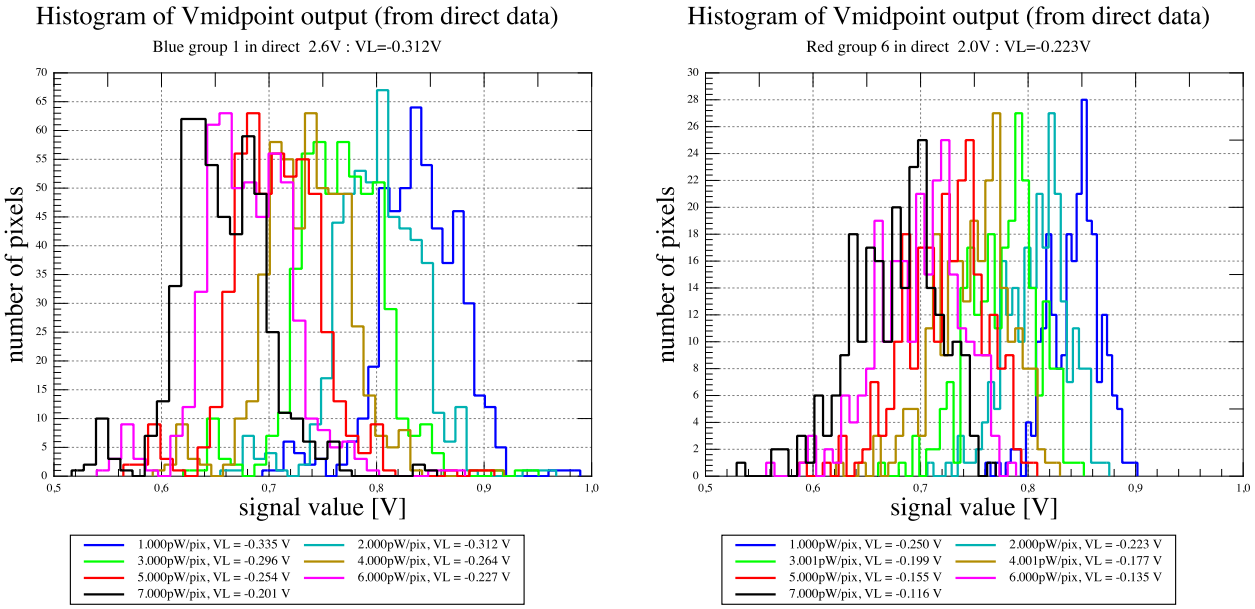

Figure 3: The distribution of V_{ptmil} observed on the two most dispersed groups of the blue (left) and red (right) array, as a function of background illumination. As the background illumination increases, the histograms shift to the left. In the legend box, we show the value of V_L that accomodates all the distribution below the upper voltage cut-off of the CL at 650 mV (i.e. we want the pixel with the highest $V_{midpoint}$ to have a V_{bolo} of 650 mv). In the subtitle we show the value corresponding to the reference background level of 2 pW/pix.

have, for all (or most pixels):

$$\begin{aligned} 650\,\mathrm{mV} &> V_{bolo} = V_L + V_{ptmil} > 250\,\mathrm{mV}, \\ 0\,\mathrm{mV} &> V_L \end{aligned} \tag{2}$$

The second line simply reminds us that on PACS, we cannot have a positive V_L. To use this condition to determine the signal range that is available to the source, we have to take into account the fact that a given background value will lead to a distribution of V_{bolo} values, as there is not a single value of V_{ptmil} for the array, but rather a distribution of these values (see Figure 3). This distribution is materialized by the blue curve on the right side of Figure 2.

Let us consider the case, quite appropriate here, of an observation of a single point source. In that case, the blue curve of Figure 2 is almost exactly the curve of Figure 3 for the appropriate background value. In particular we can consider that the maximum value of V_{ptmil} in that observation is $V^{Max}_{ptmil}(P_{bkg})$ as listed in Table 1 above. An optimal setup of the bolometer has that maximum value at the top of the CL window, i.e.:

$$650\,\mathrm{mV} = V_L + V^{Max}_{ptmil}(P_{bkg}). \tag{3}$$

From this we can obtain the optimal V_L and as long as it is negative, we can use equation (3) to substitute V_L in further computations[2].

Let us now turn to the other end of equation (2). This is where we will extract the allowed voltage range for the source. Indeed we want the V_{ptmil} of the source+background flux to be above the CL cut-off. As the V_{ptmil} value of the background is not a constant, we need to define what we consider a representative value of it, on which the source contribution will be added. The safest such value would be $V^{Max}_{ptmil}(P_{bkg}) - \Delta V_{ptmil}(P_{bkg})$, i.e. we count the source contribution from the smallest V_{ptmil} value observed in a flat configuration. This however is a bit extreme: it results in the smallest voltage range available for sources, and is strongly dependent on the distribution of outlier pixel properties. We shall therefore define a number f_{CL} between 0 and 1 and consider that the source contribution typically has to be counted on a pixel with a middle point value of $V^{Max}_{ptmil}(P_{bkg}) - f_{CL} \times \Delta V_{ptmil}(P_{bkg})$. Thus the left part of equation (2) can now be expressed as:

$$V_L + V^{Max}_{ptmil}(P_{bkg}) - f_{CL} \times \Delta V_{ptmil}(P_{bkg}) - V^{Src}_{ptmil} = 250\,\mathrm{mV}, \tag{4}$$

where V^{Src}_{ptmil} is that part of the middle point voltage contributed by the source, and the negative sign simply indicates that increasing the incoming flux (i.e. adding a source to the background) decreases the middle point voltage. Then using equation (3) we can write:

$$V^{Src}_{ptmil} = 400\,(\mathrm{mV}) - f_{CL} \times \Delta V_{ptmil}(P_{bkg}). \tag{5}$$

The choice for f_{CL} should be dictated by how safe we want to be with respect to actual saturation. For instance with $f_{CL} = 0.9$ there is a one in ten "chance" that a source with a flux just below the computed CL saturation limit still actually saturates. We personnally consider it a reasonable configuration.

It is interesting that the saturation condition apparently no longer requires knowledge of the actual value of V_{ptmil}. Equation (5) simply states that a fraction of the fixed CL dynamical range is occupied by the background dispersion. However the substitution we have made to produce equation (5) has implicitely assumed that we can always adjust V_L ideally to the distribution of background values. If

[2] Although we have reasoned in the point source case to derive the optimal V_L, we shall consider that this is the optimal V_L even in the extended source case.

that is not the case, i.e. there is no negative V_L value that satifies equation (3), then the expression for the left side of equation (2) becomes:

$$V_{ptmil}^{Src} = 250\,(\mathrm{mV}) + V_{ptmil}^{Max}(P_{bkg}) - f_{CL} \times \Delta V_{ptmil}(P_{bkg}), \tag{6}$$

because the optimal value of V_L in that case is 0 V.

Note that there is another case where we cannot use equation (3) to substitute for V_L in the saturation condition: when the value of V_L is set by an external constraint. We explore this situation in Appendix A.

With these equations, and the data of Table 1, we can now compute the voltage range accessible to sources other than the background. Numerical values corresponding to $f_{CL} = 0.9$ are collected in Table 2. Since it is a by-product of the computation, this table also lists the value of V_L that allows the corresponding source range.

Table 2: The available signal range for sources to avoid CL saturation, as a function of background, with a choice of $f_{CL} = 0.9$. We also list the corresponding value of V_L which is obtained in the course of the CL saturation derivation.

Background level (pW/pix)	Blue side V_{ptmil}^{Src} (V)	Blue side V_L (V)	Red side V_{ptmil}^{Src} (V)	Red side V_L (V)
1.0	0.151	-0.335	0.280	-0.250
2.0	0.136	-0.312	0.257	-0.223
3.0	0.121	-0.296	0.239	-0.199
4.0	0.125	-0.264	0.225	-0.177
5.0	0.109	-0.254	0.213	-0.155
6.0	0.111	-0.227	0.204	-0.135
7.0	0.113	-0.201	0.197	-0.116

3 ADC saturation

The ADC saturation is simpler to grasp as it is simply due to the fact that an analog to digital converter only has so many bits of information to store the converted signal value. This immediately defines the range of signal values it can transfer.

3.1 Gains

As far as we are concerned here, there are two possible gain values g for the AD converter: the low gain, which uses 20 μV per digital step of the converter, and the high gain, which uses 5 μV per digital step of the converter (the high gain gives you a higher resolution of the signal behavior, hence the name).

Given the 16 bits of the converter, these two gains provide a theoretically available signal range, $\Delta V_{tot}^{ADC}(g)$ of 1.31 V in low gain and 0.33 V in high gain. There is a bit more subtelty here as the ADC requires the signal to be within certain voltage limits (see RD4), but this can be accomodated through a dedicated bias (`VH_BLIND`).

Table 3: Total dispersion of the signal values (i.e. after transfer through the readout circuit, CL, but before conversion into digital values, ADC). Since we are still operating in the optimal part of the CL transfer function, we have essentially the same values as in Table 1. The difference is created by the slightly variable, non-unity, CL gain.

Background level (pW/pix)	Group 1 (blue) $\Delta V_{signal}(P_{bkg})$ (V)	Group 6 (red) $\Delta V_{signal}(P_{bkg})$ (V)
1.0	0.245	0.113
2.0	0.260	0.138
3.0	0.276	0.158
4.0	0.272	0.173
5.0	0.289	0.185
6.0	0.287	0.195
7.0	0.285	0.203

3.2 Available signal range

As we have stressed earlier, the key point is here again that eventhough great care was exercised in the matrices production to make them as uniform as possible, there still remains a large dispersion in the distribution of pixel offsets and relative gains. Thus when observing a flat flux distribution, e.g. the telescope background, we measure a very scattered distribution of signals, or, expressed in other words, a fraction of the available signal dynamical range is used, in an "irreducible" way by the telescope background, eventhough we couldn't care less about this particular signal. We have already seen the impact of this dispersion on the CL effective saturation limit, and we are now going to study its impact on the effective ADC saturation limit. For any configuration, i.e. background level, gain setting, photometer side, the actual saturation limit will be the smallest of the ADC and CL limits.

For the ADC saturation limit computation, we will use again data from the FM-ILT. These allow the computation of the maximum extent of the background signal dispersion at the entrance of the AD converter (noted $\Delta V_{signal}(P_{bkg})$ to use a notation compatible with the one developed above). To derive the signal range available for a source, V_{signal}^{Src}, we simply have to write that the total ADC range (which is a function of the gain g) is the sum of the source voltage, and of a fraction f_{ADC} of the total extent of the background dispersion. This is the same reasonning as before: we define a representative signal value of the background on which the source signal stands as $f_{ADC} \times \Delta V_{signal}(P_{bkg})$, with $f_{ADC} = 1$ corresponding to the safest situation, i.e. the source signal sits on the highest background signal. Since we have to define a single saturation limit per photometer side, we need to compute $\Delta V_{signal}(P_{bkg})$ on the most dispersed groups, which are again group 1 on the blue side and group 6 on the red side. Table 3 lists these values as a function of the background flux. For reasons that would be too long to explain here (and that are related to the fact that accessing any other quantity than the output signal is very complicated), the actual value of $\Delta V_{signal}(P_{bkg})$ depends on the gain. Values in Table 3 are derived assuming we work in low gain which is the optimistic situation (i.e. $\Delta V_{signal}(P_{bkg})$ is smaller by a few 10s of mV in low gain than in high gain, but this is purely a measure of the uncertainty associated with the determination of $\Delta V_{signal}(P_{bkg})$). This table is a bit redundant with Table 1 as what we are seeing here is only the effect of the slightly variable, and non-unity, CL gain (see RD4).

Table 3 reveals that on the blue side, much of the ADC range at high gain (0.33 V) is in fact occupied by the background dispersion alone. This is why choosing $f_{ADC} = 1$ may be the safest choice, but is at the same time a bit too restrictive. Here again we will choose a more practical value at $f_{ADC} = 0.9$. To compute the ADC saturation limit, we simply have to apply the following saturation condition:

$$V_{signal}^{Src} = \Delta V_{tot}^{ADC}(g) - f_{ADC} \times \Delta V_{signal}(P_{bkg}). \quad (7)$$

The result of applying this condition to all the values of Table 3 is listed in Table 4 which gives the available source signal range for both photometer sides, for both gain choices, as a function of background power.

Table 4: The maximum signal voltage allowed for a source in the case of ADC saturation only. These were obtained with a value of $f_{ADC} = 0.9$, on both photometer sides and for all values of the background.

Background level	V_{signal}^{Src} Blue side		V_{signal}^{Src} Red side	
	High	Low	High	Low
(pW/pix)	(V)	(V)	(V)	(V)
1.0	0.1095	1.0895	0.2283	1.2083
2.0	0.0960	1.0760	0.2058	1.1858
3.0	0.0816	1.0616	0.1878	1.1678
4.0	0.0852	1.0652	0.1743	1.1543
5.0	0.0699	1.0499	0.1635	1.1435
6.0	0.0717	1.0517	0.1545	1.1345
7.0	0.0735	1.0535	0.1473	1.1273

Table 4 already shows that a factor of 4 change in the gain has a much more dramatic effect on the ADC range available for sources: this is because we move from a situation where most of the dynamical range is used by the background (high gain) to one where most of the dynamical range can be used by sources (low gain). This must however immediately be mitigated by the fact that in the second situation, we will very likely see CL saturation before we reach ADC saturation. This is what we are going to find out immediately.

4 Turning a voltage range into a source flux

4.1 From Volts to Watts

As mentioned above, for each combination of (P_{bkg}, gain, photometer band), the maximum voltage value available for the source is given by the smallest value of Tables 4 and 2 for that combination. For the sake of this document's clarity, we list these effective maximum signal values in Table 5 but remember that they heavily depend on (arbitrary) choices of f_{CL} and f_{ADC} (both at 0.9). What is immediately striking in this table is that the effect of the gain is almost cancelled: switching from high to low gain "opens" the source dynamical range by less than a factor 2. This is because at low gain, we are dominated by the effect of CL saturation which happens much before we reach ADC saturation.

Table 5: The maximum signal voltage allowed for a source taking into account both the ADC and CL saturation limits. This is a result obtained by taking for each configuration, i.e. bagkground flux, ADC gain, and photometer band, the smallest source signal allowed by ADC saturation or CL saturation. As can be seen, taking both ADC and CL into account changes quite drastically the (mis)-conception that the low gain allows a much larger dynamical range. At high gain, we are dominated by the ADC saturation, while at low gain we are dominated by CL saturation.

Background level	V^{src} Blue side		V^{Src} Red side	
	High	Low	High	Low
(pW/pix)	(V)	(V)	(V)	(V)
1.0	0.110	0.151	0.228	0.280
2.0	0.096	0.136	0.206	0.257
3.0	0.082	0.121	0.188	0.239
4.0	0.085	0.125	0.174	0.225
5.0	0.070	0.109	0.164	0.213
6.0	0.072	0.111	0.155	0.204
7.0	0.074	0.113	0.147	0.197

We now need to turn these voltage values into power values, in pW/pix. To do this properly we need to take into account the fact that the responsivity is a function of the background level (i.e. the non-linearity of the bolometers). In a first approximation, to convert the available signal range in an avalaible power range, we can simply use the reponsivity measured at the chosen background level. However to be more accurate, we should take into account the fact that the source power itself can modify the response. This is specially true when the available source range is large. For either of these choices, we need to have the evolution of the response with incoming power, for both sides of the photometer. This has been measured in FM-ILT (and curves showing the variation of the response are available in RD2) and to those measurements, we have fitted a function to represent the responsivity curve $R(p)$, were p is an abitrary value of the background flux, in W/pix, while R is in V/W. With some elementary maths, one can show that the signal elevation Δs (in V) created by a power increase Δp over a background p (both in pW/pix) are related by:

$$\Delta s = \int_{p}^{p+\Delta p} R(p)\, dp. \tag{8}$$

In our case Δs is what we know, i.e. the available signal range over the dynamical range reserved for the background values, and what we are looking for is Δp.

In order to compute the saturation limits, we first fitted the non-linear response by a second order poynomial ($R(p) = \sum_0^2 a_i p^i$) but this leads to problems as this kind of fit only works close to the sampled background flux values, while, at low gain, we can observe sources that are strong enough that we in fact depart significantly from the sampled values. The typical problem is that at high p, the fit shows the response increasing again, while this is physically impossible. A better fitting function is $R(p) = \sum_0^3 a_i \times (\log p)^i$. This also has problems: at high values of p the response is so low that it is impossible to get a significant increase in signal. This is however much closer to the actual behavior (saturation of the response) than what a simple polynomial fit on $R(p)$ would give. In Table 6 we list the 4 coefficients of the fit for the blue and red sides.

Table 6: Coefficients for the non-linear response fit ($R(p) = \sum_0^3 a_i \times (\log p)^i$), with log representing the decimal logarithm, performed on FM-ILT measurements (see RD2). These coefficients assume that p is in W/pix and $R(p)$ is in V/W. Note that because of the log function and of the absolute values of the variables, it is essential to keep that many significant digits on the coefficients. In order to get a reasonable behavior for the response at high incoming power, an artificial very low response value at very high flux was introduced in the fit.

Side	a_0	a_1	a_2	a_3
Blue	$+5.00281\,10^{12}$	$+1.39854\,10^{12}$	$+1.28891\,10^{11}$	$+3.90653\,10^{9}$
Red	$+1.28632\,10^{13}$	$+3.51174\,10^{12}$	$+3.17365\,10^{11}$	$+9.48121\,10^{9}$

Thus, using these fits, one can derive the limiting value of W/pix from source signal that we can accomodate between the fraction of the dynamical range that has to be reserved for the background, and the 250 mV limit imposed by the CL or the cutoff of the ADC range (i.e. Table 5). A small IDL code is used to do just that and the results of this code are presented in Table 7. This table shows quite convincingly that "saturation" of the PACS bolometer arrays is conceptually different from that of a photo-detector.

For instance on the blue side, we see that the saturation limit first goes down with background level and then increases again[3]. This is because we have a competition between the decreasing voltage range available for sources as the background flux increases, and the rapid decrease of the response with background (which "requires" more flux to produce the same voltage output at high background level). This competition is different on the red side and thus the trend reversal does not occur at the same location. Furthermore, because the signal range is determined differently at high and low gain (respectively ADC and CL saturation), this introduces a further difference between the high and low gain maximum power trend with background.

Finally, now that we are back into more friendly units, one can see that there is not a drastic evolution of the saturation limit with background level. This may sound surprising but this is due to the decrease of the response at high background level that compensates the closure in signal range. One should remember that a drop in response is accompanied by a decrease in sensitivity so this "nice" feature also comes with a drawback. We also see that switching from high to low gain will allow an increase of a factor of ≤ 2 in saturation limit, not a factor of 4 as could be expected from the gain ratio.

Once again, one should remember that obtaining these numerical values requires making choices for how one wants to handle the intrinsic dispersion of the arrays (f_{CL}, f_{ADC}). Theses figures were obtained with $(f_{CL}, f_{ADC}) = (0.9, 0.9)$.

4.2 From Watts to Janskys

The final step is to convert that power into a source (point or extended) flux density. To perform that transformation we use the formalism developed in RD3 for the background power computation. Although they are quite similar, we will distinguish the point source case from the extended source case. In both cases however, we will assume that $f_\nu^{src} \propto \nu^{-1}$, which is the PACS photometric convention.

[3]There is a "glitch" on this trend at 4 pW/pix. This is visible in Table 5 and is likely due to our use of the maximum extent of the background distribution. Even if we exclude the masked pixels, this makes us dependent on the extreme values of the distribution, which may sometimes show a deviant behavior.

Table 7: The maximal source power (in pW/pix) that can be accomodated within the saturation limits of the ADC and CL in the high and low gain (see text for comments). These limits where obtained assuming $(f_{cl}, f_{ADC}) = (0.9, 0.9)$, see text for details.

background	Signal range - Blue side		Signal range - Red side	
	High	Low	High	Low
(pW/pix)	(pW/pix)	(pW/pix)	(pW/pix)	(pW/pix)
1.0	4.509	6.736	9.387	13.322
2.0	4.285	6.581	9.375	13.569
3.0	3.895	6.228	9.447	14.031
4.0	4.457	7.028	9.675	14.637
5.0	3.839	6.469	9.991	15.394
6.0	4.245	7.092	10.369	16.406
7.0	4.669	7.741	10.853	17.656

For a point source (where f_ν^{src} is expressed in W.m^{-2}.Hz^{-1}), the power (in W) collected per telescope beam can be written in the following way:

$$P^{src} = \int_{-\infty}^{+\infty} A_{tel}\, t_{mir}\, t_{Lyot}\, \eta_{prop}\, t_{filt}(\nu)\, f_\nu^{src}\, d\nu, \tag{9}$$

where A_{tel} is the telescope collecting surface, t_{mir} is the total mirror transmission, t_{Lyot} is the transmission of the Lyot stop, η_{prop} captures various uncertainties and subtleties in the propagation of light through the optical system, $t_{filt}(\nu)$ is the absolute filters and dichroic transmission curve[4]. We refer the intrigued reader to RD3 for lengthy dicussions of these parameters. Their numerical values are extracted from RD3 and listed in Table 8. In principle there should also be a telescope efficiency parameter that describes how much of a point source flux actually makes it to the main beam of the telescope, but as can be seen from RD3, quantifying this is still beyond our reach and we have set this efficiency to 1.

For each of the photometer band, denoted by the index i, f_ν^{src} can be written as $f_{\nu_0^i}^{src} \times (\nu_0^i/\nu)$ and thus we have:

$$f_{\nu_0^i}^{src} = P_i^{src} \times \frac{1}{A_{tel}\, t_{mir}\, t_{Lyot}\, \eta_{prop} \int_{-\infty}^{\infty} t_{filt,i}(\nu)\, (\nu_0^i/\nu)\, d\nu} \tag{10}$$

For point sources, only a fraction $f_i^{psf} < 1$ of the power per beam falls in the central pixel, therefore, noting P_i^{pix} the power per pixel falling in the central pixel (i.e. the values computed in Table 7) we can finally express the maximum point source flux as a function of the allowed power range per pixel as:

$$f_{\nu_0^i}^{src} = \frac{P_i^{pix}}{f_i^{psf}} \times \frac{1}{A_{tel}\, t_{mir}\, t_{Lyot}\, \eta_{prop} \int_{-\infty}^{\infty} t_{filt,i}(\nu)\, (\nu_0^i/\nu)\, d\nu} \tag{11}$$

The values of f_i^{psf} have been computed theoretically and are also shown in Table 8.

[4]Note that it should also include the detector absorption efficiency to be formally correct, but this had not been included in the conversion factors used during ILT. For internal consistency we have chosen to continue in this erroneous path.

Table 8: Numerical values for the parameters used in the power-to-flux-density conversion computations. These values are copied from RD3 where an extensive discussion of their signification can be found (when the value is "author-dependent" we have chosen the MS scenario). Central frequencies refer to the Müller definition for the PACS bands, i.e. 70, 100 and 160 μm. The fraction of a PSF flux that falls in the central pixel is a theoretical computation.

Parameter	Blue	Green	Red
A_{tel} (m^2)	8.48		
t_{mir}	$0.99^{16} = 0.85$		
t_{Lyot}	0.95		
η_{prop}	1.04		
ν_0^i (10^{12} Hz)	4.29	3.00	1.76
f_i^{psf}	0.310	0.165	0.250
Ω_i^{pix} (10^{-10} sr)	2.38	2.38	9.52

In the extended source case, (where f_ν^{src} is now expressed in $W.m^{-2}.Hz^{-1}.sr^{-1}$), the power (in W/pix) collected per pixel can be written in the following way:

$$P^{src} = \int_{-\infty}^{+\infty} \Omega_i^{pix}\, A_{tel}\, t_{mir}\, t_{Lyot}\, \eta_{prop}\, t_{filt}(\nu)\, f_\nu^{src}\, d\nu, \tag{12}$$

where Ω_i^{pix} is the detector pixel's solid angle. As P^{src} is expressed in W/pix, this is exactly the quantity computed in Table 7 and thus, using the same notations as in the point source case, we have:

$$f_{\nu_0^i}^{src} = \frac{P_i^{pix}}{\Omega_i^{pix}} \times \frac{1}{A_{tel}\, t_{mir}\, t_{Lyot}\, \eta_{prop} \int_{-\infty}^{\infty} t_{filt,i}(\nu)\, (\nu_0^i/\nu)\, d\nu} \tag{13}$$

Thus we only need to integrate the filter transmission curves, chosen here as the cold FM filters plus warm dichroic (in conformance with RD3) to convert the power limits of Table 7 into saturating source fluxes. These numbers are collected in Table 13 for the three bands, at different backgroud levels and for the two settings of the ADC gain. For practical reasons, this table can be found at the last page of this document.

5 Closing comments

In this section we compile a list of remarks generated by the diffusion of this document to a broader circle.

- **Can saturation of a pixel affect a neighboring pixel?** In principle the answer is no. Unlike a CCD there is no transfer of information from one pixel to the next so the fact that a pixel is saturated should not affect a neighboring pixel in any way. However one must realize that since we resolve our PSF, it is unlikely that in the case of a saturating point source, only one pixel would be saturated. But again, this is not an influence from one pixel to the next. Still on this issue, we have observed that very sharp illumination contrast can lead to crosstalk between two pixel on the same output line (long axis of the photometer). It remains to be investigated whether we can isolate this effect in the case of a saturating point source. However again, this is not a "bleeding" of a saturating pixel on its neighbor.

- **When do we reach the non-linear regime?** This question probably stems from early presentation of the PACS bolometers, when even us had unclear ideas regarding their behavior. The PACS bolometers are intrisically non-linear detectors. This is demonstrated by the fact that to fit the behavior of the response, we need a third order polynomial fit on $\log(p)$. Therefore there is no such thing as a linear regime for the bolometers. That being said, the bolometers are only midly non-linear which means that at any point the response curve can be approximated by a straight line, provided one is willing to accept a finite error on the response.

- **Aren't the saturation limits a bit pessimistic?** Yes they are. The principal advantage of being pessimistic is that you see the problems very early on, which is important when you are in charge of an observatory. Thus indeed there is a high probability that someone observing a source at the saturation limit will turn out quite fine (for instance if it happens to fall on a pixel that is on the low part of the background V_{ptmil} distribution). This will be a nice surprise. The saturation limit could be increased by tuning the detectors in such a way (i.e. with V_L) that the lowest background pixels are above the high cut of the CL. This however assumes that these pixels are deviant, which is not necessarily the case, and furthermore, once the detector is tuned this way, those pixels are rendered useless for all observers. We do not feel that it is a fair trade to diminish the sensitive area for all observers for the sake of a relatively small number of observers whishing to observe very bright sources. There is an alternate solution for these observers (mostly calibration scientists): make sure that their source falls on the matrix that has the smallest dispersion, which is matrix 7 on the blue side (see appendix B).

Appendices

A A single setup for the blue and green filters, and its consequences

As explained before, we have assumed that we can set up the instrument differently for blue and green filter observations (i.e. we can adapt the value of V_L and `VH_BLIND` to the different background level seen in these two filters). This is feasible but this is not the current baseline for the photometer operations. We examine in this appendix the consequence of having only one setup for the blue side. To avoid adding too much material to this already long report, we shall only do this for a single configuration of the background. In RD3 we computed likely values for the background flux in all three filters of the photometer. These were 2.75 pW/pix for the blue filter, and 1.54 pW/pix for the green filter. For simplicity's sake, let us now assume that the background stands at 3.0 pW/pix and 2.0 pW/pix for the blue and green filters respectively.

For the CL saturation limit, V_L is now set by the maximum middle point values observed at the two flux levels (equation 3). From Table 1 we find that this is 0.962 V obtained for a 2.0 pW/pix flux. Thus the value of V_L we will have to use for both filters is $V_L = -0.312$ V, and this is the optimal value for the green filter, not for the blue filter. This means that the CL saturation limit is unchanged for the green filter (it is that quoted for the 2.0 pW/pix background flux), but we have to recompute it for the blue filter. We use equation (4) with the predefined value of $V_L = -0.312$ V. This gives us a saturation limit in the blue filter of 0.105 V, to compare to 0.121 V when V_L could be optimally adjusted.

Let us now turn to the ADC. In the main part of this report we have not discussed the role of `VH_BLIND` because the optimal adjustment of V_L to the observed background distribution leads to a constant

VH_BLIND value as a function of the background[5].

Since V_L is optimal for the green filter, and the distribution of V_{bolo} for the background in the blue filter is shifted toward lower values, it turns out that we have to keep VH_BLIND at its original value (i.e. optimized for the green filter) if we want to fit all the green background points in the ADC window. The result of this is that (1) for the green filter nothing changes, and (2) for the blue filter, since the signal is now shifted to slightly higher values with respect to the green filter (remember the signal we code is proportional to VH_BLIND$-V_{bolo}$), a fraction of the ADC window (at the bottom) will be left unoccupied. Therefore the source range will be smaller. To compute it we simply need to realize that the effective range of values reserved by the background in the blue case is no longer $\Delta V_{Signal}(3\,\mathrm{pW/pix})$ but rather $V_{Signal}^{Max}(3\,\mathrm{pW/pix}) - V_{Signal}^{Min}(2\,\mathrm{pW/pix})$. This stands at 0.291 V. We can now use equation (7) to compute the available source range and this is 0.0681 V in high gain, and 1.0481 V in low gain (to compare to the original values of 0.0816 V and 1.0616 V). So we see that the ADC limit has also changed. Combining both CL and ADC limits gives new saturation limits for the blue filter (the green limits are unchanged) of 0.068 V in high gain and 0.105 V in low gain (to compare to the original values of 0.082 V and 0.121 V).

Let us now express these limits into units that make more sense to calibration scientist and astronomers. First we convert these signal levels into power per pixel, remembering that we are making our computation on a blue background level of 3.0 pW/pix. Using the tabulated response function (Table 6) we obtain power limits of 3.169 and 5.241 pW/pix for the blue filter in respectively high and low gain (to be compared with the values of 3.895 and 6.228 pW/pix for an optimal setting, Table 7). Finally we convert these power values into source flux densities, following Section 4.2. Because this is now a large number of values, and making them noticeable is important, I list them in Table 9 along with the limits corresponding to an optimal setup for the blue filter.

The decrease in saturation limit is quite significant, and could justify that we modify the operational baseline for the photometer. Given that an AOR cannot mix the blue and green filters, this is quite feasible. The preamble of the AOR could include a setting of the biases optimial for the chosen filter. This is very fast and the stabilization time after the bias change is only of a few seconds. This requires however a decision by the ICC as this will have a significant impact on the operation sofwtare.

Table 9: Saturation limits in the blue filter for a single setting of the blue photometer (i.e. corresponding to the optimal setting for the green filter). The second line of the table corresponds to the blue limits for an optimal setting (these are just copied from Table 13). In extended source case, we quote the limit both in Jy/"^{2} and in MJy/sr to accomodate all tastes in extended flux units.

Background level	High gain			Low gain		
	PS	ES		PS	ES	
(pW/pix)	(Jy)	(Jy/"^{2})	(MJy/sr)	(Jy)	(Jy/"^{2})	(MJy/sr)
Blue band - Single setting						
3.0	214	6.58	2.8e+05	355	10.88	4.6e+05
Blue band - Optimal setting						
3.0	264	8.09	3.4e+05	422	12.93	5.5e+05

[5]This is because the optimal choice of V_L places the maximum value of the distribution of V_{bolo} (i.e. the minimum background signal) at 650 mV. As we use VH_BLIND to ensure that VH_BLIND$-V_{bolo}$ fits into the ADC window, VH_BLIND is set by the signal value corresponding to $V_{bolo} = 650$ mV. It is therefore independent of the background level as long as V_L can be optimally set.

Finally one may wonder why we use as a single setting the one which is optimal for the green filter, while Table 13 show that the saturation limit is always larger for the green filter than for the blue. Couldn't we do the opposite: stay optimal for the blue and compromise for the green? The short answer is no. The long answer is that the saturation limit is entirely fixed by the background level: as for any reasonable configuration of the telescope, it will be smaller in the green filter than in the blue filter, the highest background V_{ptmil} will be observed for the green filter, hence this filter defines the setting. Choosing the optimal setting for the blue would mean that we saturate on the background for the green (and *this* will be hard to explain to observers), i.e. some of the pixels seeing the background in the green filter will give a V_{ptmil} higher than 650 mV and their signal will not be carried through the CL.

B Limits for the most tolerant blue areas: group 2 and matrix 7

In all this document, we have used relatively pessimistic assumptions in order to arrive at conservative source fluxes for the saturation limit. This choice was made because it is the safest in the context of observatory management. However the values of Table 13 immediately show that some very interesting calibration sources cannot be observed, specially at short wavelengths.

Regarding calibration observations, we know that calibration scientists can have much more control on source placement on the array or on the observation strategy than regular observers. We can exploit that. We know that not all the groups show the same dispersion (see Figure 1), and group 2 has the smallest dispersion of V_{ptmil} observed. We also know that some matrices are very homogenous, apart from a few pixels on their edges and among them, matrix 7 is the best behaved (i.e. most of its central area is very homogenous). With an AOR such as the small source one, it is feasible to keep the target on the same group or even on the same matrix[6] for the whole observation. In that case, the general saturation limits are too pessimistic. Let us thus assume that an observation of a bright source can be made such that either the source is always on group 2, or the source is always in the central area of matrix 7. What would be the saturation limits then?

The first item that needs updating is the CL limit, because we are now focusing on a group with a much smaller dispersion. On Figure 4 we show the histograms of V_{ptmil} for group 2 as a whole and matrix 7. There are already narrower than our worst case (group 1), and when the few pixels in the low V_{ptmil} tail of matrix 7 are discarded, the dispersion can indeed be very narrow (these tail pixels are on the edges of matrix 7 thus their saturation will not prevent a point source observation). In Table 10, we list the values of $\Delta V_{ptmil}(P_{bkg})$ and $V_{ptmil}^{Max}(P_{bkg})$ observed for group 2 and the main peak of matrix 7.

From Table 10, and following the approach of Section 2.2 (i.e. $f_{CL} = 0.9$) we can compute the source signal values that will saturate group 2 or the central area of matrix 7, and we report those as well in Table 10 (in **boldface**). These are already significantly different from the reference values (see Table 2). For instance on matrix 7 we have an available range which is twice as large as the reference range, and on group 2 the increase is of the order of 50-70%. It is very important to realize that no special setup is required here. For group 2, since we are measuring the whole dispersion of the group, we are applying no special conditions for its setup. For matrix 7 the situation could be different in principle, as an optimal setup for one matrix in a group is generally not optimal for the other matrix, however we are in a particular situation here since the highest V_{ptmil} value for group 4 is on matrix 7, thus the optimal group 4 setting is in fact defined by matrix 7 (in fact, the two matrices of group 4 are very distinct and most of the pixels in matrix 7 have a V_{ptmil} higher than those observed on

[6] with a small modification of the AOR parameters.

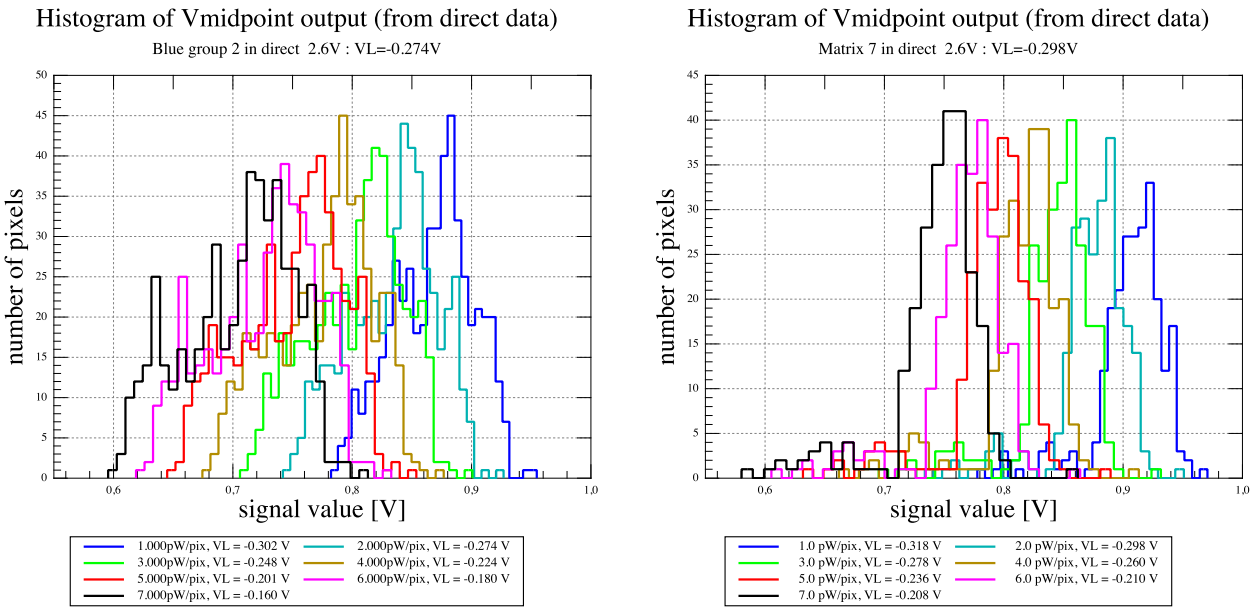

Figure 4: The V_{ptmil} histograms for the areas with smallest dispersion: group 2 (left) and matrix 7 (right). Matrix 7 has a tail of "bright" pixels that we will ignore in our computation as they are located on the edges of the area. Comparison of these histograms with Figure 3 show that there will be a noticeable gain on the CL limit.

matrix 8). Thus here again, no special setup is required to allow the saturation limits we will derive in this appendix.

Let us now turn to the ADC saturation condition. Here again we see the same behavior, i.e. that as a group, group 2 is the one with the smallest dispersion of signal values, while most of the central area of matrix 7 is extremely homogenous. In Table 11 we thus list, similarly to Table 3, the values of ΔV_{signal} as a function of P_{bkg} for both the whole of group 2 and the main peak of matrix 7. Following the formalism exposed in Section 3.2 (i.e. using $f_{ADC} = 0.9$) we can use these dispersion values to compute the available signal range allowed by the ADC, V_{signal}^{Src} and we report those values in Table 11 as well. As can be seen from a comparison with Table 3 the change is here as well noticeable, with an increase by a factor of 2-2.5 of the available source signal range.

Now that both the CL and ADC available source ranges are defined, we can compute, in each gain configuration the effective source range available (the smallest of the two), convert that into an incident power using the tabulated response curve of the blue array, and then, using the blue and green filter transmission curves, compute the correponding point source and extended source saturation limits following the formalism of Section 4. These are listed in Table 12. Comparing Table 12 to the reference one (Table 13) shows how large the impact can be of knowing where you source will fall on the array. In a scanning mode observation it is hopeless to think that one could control the observation parameters accurately enough to make sure that the bright sources fall on the most forgiving areas of the blue photometer. In the point source AOR, we require the source to fall on each group so here again, we have to use the baseline saturation levels. However in the small source AOR, we can, through an educated choice of the pointing, make sure that the sources stay on these regions of the photometer. Therefore there is a way to observe even the brightest calibration source (e.g. Uranus)

Table 10: Total dispersion of the middle point values observed on group 2 (whole group) and on matrix 7 (only the main peak) as a function of background illumination, accompanied by the maximum observed middle point value on these groups. In this table we also list, in **boldface** the corresponding voltage range available for sources (computed with $f_{CL} = 0.9$) as well as the value of V_L that allows this range.

Background level (pW/pix)	Group 2 (all) ΔV_{ptmil} (V)	V_{ptmil}^{Max} (V)	V_{ptmil}^{Src} (V)	V_L (V)	Matrix 7 (main peak) ΔV_{ptmil} (V)	V_{ptmil}^{Max} (V)	V_{ptmil}^{Src} (V)	V_L (V)
1.0	0.162	0.952	**0.254**	-0.302	0.100	0.968	**0.310**	-0.318
2.0	0.173	0.924	**0.244**	-0.274	0.113	0.948	**0.298**	-0.298
3.0	0.183	0.898	**0.235**	-0.248	0.131	0.928	**0.282**	-0.278
4.0	0.190	0.874	**0.229**	-0.224	0.150	0.910	**0.265**	-0.260
5.0	0.196	0.851	**0.224**	-0.201	0.146	0.886	**0.269**	-0.236
6.0	0.200	0.830	**0.220**	-0.180	0.125	0.860	**0.287**	-0.210
7.0	0.204	0.810	**0.216**	-0.160	0.146	0.858	**0.269**	-0.208

with the photometer. We recall that this requires no special setup of the photometer so that there would be no continuity break in the calibration chain.

A potentially intriguing feature of Table 12 is the small effect of the gain: switching from high to low gain only increases the saturation limits by $\sim 30\%$ when the gain change is a factor of 4. This is not a mistake. The fact that the intrinsic dispersion has decreased has opened the source range quite drastically and now this range is almost identical at the CL level and at the ADC level in high gain (this was not the case when the background dispersion was larger, the CL source range was about 50% larger than the high gain ADC source range). Since at low gain, as before, we are under a CL saturation regime while at high gain we are under an ADC saturation regime, the fact that the two ranges are much closer than before results in a very small difference in effective saturation limit between high and low gain.

Table 11: Total dispersion of the signal values (i.e. after transfer through the readout circuit, CL, but before conversion into digital values, ADC), along with the corresponding source range allowed (assuming $f_{ADC} = 0.9$) in high, then low gain.

Background level	Group 2 (all)			Matrix 7 (main peak)		
	$\Delta V_{signal}(P_{bkg})$	V_{signal}^{Src}		$\Delta V_{signal}(P_{bkg})$	V_{signal}^{Src}	
		High	Low		High	Low
(pW/pix)	(V)	(V)	(V)	(V)	(V)	(V)
1.0	0.131	**0.2121**	**1.1921**	0.072	**0.2652**	**1.2452**
2.0	0.143	**0.2013**	**1.1813**	0.082	**0.2562**	**1.2362**
3.0	0.151	**0.1941**	**1.1741**	0.091	**0.2481**	**1.2281**
4.0	0.158	**0.1878**	**1.1678**	0.112	**0.2292**	**1.2092**
5.0	0.164	**0.1824**	**1.1678**	0.108	**0.2328**	**1.2128**
6.0	0.169	**0.1779**	**1.1579**	0.108	**0.2328**	**1.2128**
7.0	0.172	**0.1752**	**1.1552**	0.119	**0.2229**	**1.2029**

Table 12: Saturation limits for **group 2** and for the **main peak of matrix 7**, showing only the blue and green filters, as the red filter is unaffected. For each of the filter band, we show the limits as a function of the background level, in the high and low gain case, for point and extended source. In the case of extended source, we quote the limit both in Jy/"^{2} and in MJy/sr. **These are not the reference saturation limits.**

Background level	High gain			Low gain		
	PS	ES		PS	ES	
(pW/pix)	(Jy)	(Jy/"^{2})	(MJy/sr)	(Jy)	(Jy/"^{2})	(MJy/sr)
Group 2 (all) Blue band						
1.0	728	22.28	9.5e+05	952	29.16	1.2e+06
2.0	750	22.97	9.8e+05	996	30.51	1.3e+06
3.0	783	23.98	1.0e+06	1036	31.72	1.3e+06
4.0	815	24.96	1.1e+06	1086	33.25	1.4e+06
5.0	848	25.96	1.1e+06	1138	34.84	1.5e+06
6.0	883	27.03	1.2e+06	1201	36.77	1.6e+06
7.0	928	28.42	1.2e+06	1262	38.65	1.6e+06
Group 2 (all) Green band						
1.0	1693	27.59	1.2e+06	2215	36.10	1.5e+06
2.0	1745	28.44	1.2e+06	2317	37.76	1.6e+06
3.0	1822	29.69	1.3e+06	2410	39.27	1.7e+06
4.0	1896	30.90	1.3e+06	2526	41.16	1.8e+06
5.0	1972	32.14	1.4e+06	2647	43.13	1.8e+06
6.0	2054	33.47	1.4e+06	2793	45.52	1.9e+06
7.0	2159	35.19	1.5e+06	2936	47.85	2.0e+06
Matrix 7 (main peak) Blue band						
1.0	1017	31.15	1.3e+06	1314	40.23	1.7e+06
2.0	1072	32.83	1.4e+06	1373	42.05	1.8e+06
3.0	1123	34.40	1.5e+06	1381	42.30	1.8e+06
4.0	1088	33.30	1.4e+06	1366	41.82	1.8e+06
5.0	1210	37.05	1.6e+06	1524	46.66	2.0e+06
6.0	1310	40.12	1.7e+06	1872	57.31	2.4e+06
7.0	1321	40.45	1.7e+06	1801	55.13	2.3e+06
Matrix 7 (main peak) Green band						
1.0	2366	38.56	1.6e+06	3057	49.81	2.1e+06
2.0	2494	40.64	1.7e+06	3195	52.06	2.2e+06
3.0	2613	42.58	1.8e+06	3213	52.36	2.2e+06
4.0	2530	41.23	1.8e+06	3177	51.77	2.2e+06
5.0	2815	45.87	2.0e+06	3545	57.76	2.5e+06
6.0	3048	49.66	2.1e+06	4354	70.95	3.0e+06
7.0	3073	50.08	2.1e+06	4189	68.25	2.9e+06

Table 13: **The baseline source flux saturation limits**. For each of the filter band, we show the limits as a function of the background level, in the high and low gain case, for point and extended source. In the case of extended source, we quote the limit both in Jy/"^{2} and in MJy/sr to accomodate all tastes in extended flux units.

Background level	High gain			Low gain		
	PS	ES		PS	ES	
(pW/pix)	(Jy)	(Jy/"^{2})	(MJy/sr)	(Jy)	(Jy/"^{2})	(MJy/sr)
Blue band						
1.0	305	9.36	4.0e+05	456	13.99	6.0e+05
2.0	290	8.90	3.8e+05	446	13.67	5.8e+05
3.0	264	8.09	3.4e+05	422	12.93	5.5e+05
4.0	302	9.26	3.9e+05	476	14.59	6.2e+05
5.0	260	7.97	3.4e+05	438	13.43	5.7e+05
6.0	287	8.81	3.8e+05	481	14.73	6.3e+05
7.0	316	9.69	4.1e+05	525	16.07	6.8e+05
Green band						
1.0	711	11.59	4.9e+05	1062	17.32	7.4e+05
2.0	676	11.02	4.7e+05	1038	16.92	7.2e+05
3.0	614	10.01	4.3e+05	982	16.01	6.8e+05
4.0	703	11.46	4.9e+05	1108	18.07	7.7e+05
5.0	605	9.87	4.2e+05	1020	16.63	7.1e+05
6.0	669	10.91	4.6e+05	1119	18.23	7.8e+05
7.0	736	12.00	5.1e+05	1221	19.90	8.5e+05
Red band						
1.0	1284	7.93	3.4e+05	1823	11.25	4.8e+05
2.0	1283	7.92	3.4e+05	1857	11.46	4.9e+05
3.0	1293	7.98	3.4e+05	1920	11.85	5.0e+05
4.0	1324	8.17	3.5e+05	2003	12.36	5.3e+05
5.0	1367	8.44	3.6e+05	2107	13.00	5.5e+05
6.0	1419	8.76	3.7e+05	2245	13.86	5.9e+05
7.0	1485	9.17	3.9e+05	2416	14.91	6.3e+05